These provocation tests confirmed that all 10 patients had FDEIA.

Skin testing, histamine release tests, and IgE measurement

To verify the effects of aspirin on accelerating histamine release from mast cells/basophils, we carried out SPTs and *in vitro* HRTs (release from basophils) prior to and after aspirin intake (Table SI). Specific IgE antibodies against the causative food allergens were detected in nine of the 10 patients with FDEIA in the study. The SPTs with the causative allergens were not enhanced after aspirin intake in patients 1, 3, 6, 8, or 10. SPTs with gluten and bread were enhanced after aspirin intake in patients 5 and 7. Hence, the skin tests with causative food allergens were not enhanced by pretreatment with aspirin in 5 of the 7 patients tested. Administration of aspirin just before food intake, but not exercise after food intake, induced FDEIA symptoms only in patients 5 and 7, in whom the skin tests were enhanced.

HRTs with causative food allergen extracts were performed in all 10 patients with FDEIA prior to and after aspirin intake. Because anti-IgE antibodies could not induce enough histamine release from the basophils in patient 10, she was deemed a non-responder, and hence the HRT could not be assessed. There was significant histamine release from the basophils of all patients except patient 10 with each causative food allergen extract before aspirin intake. Histamine release with the causative food allergen did not increase significantly after aspirin intake compared with that before aspirin intake in 8 of 9 patients. In patient 6, histamine release was increased by the bread extract at a dilution of 1:1000, but at 1:10 and 1:100 dilutions the response was deemed negative and the increase was not significant.

DISCUSSION

Ingestion of a suspected food alone did not provoke symptoms in any of the patients in this study. In 4 of the 10 (40%) patients, the combination of food and exercise did induce symptoms. In contrast, the addition of aspirin induced positive provocation tests in 7 of the 9 patients tested. Similar to previous reports (15), the combination of food and exercise alone was not enough to diagnose FDEIA using provocation tests. Aspirin, a definitive factor for aggravating symptoms in patients with FDEIA, may therefore be a powerful tool for establishing a precise diagnosis of FDEIA. In contrast, the independent addition of exercise or aspirin to the food challenge induced symptoms only in patient 3. Thus, the aggravation factors may play different roles and functions in patients with FDEIA depending on the individual patient.

Few reports have documented the usefulness of HRTs in diagnosing FDEIA (15, 23). Currently, HRTs with basophils from a patient are not commonly used to diagnose FDEIA. In the present study, HRTs with an appropriately diluted extract of the particular food allergen were positive in all of the patients with FDEIA. The respective food allergen extract was used as an appropriate antigen for the HRTs because most of the extracts elicited positive skin tests. When the dilution of the extract was inappropriate (too concentrated, or too diluted), suitable results were not acquired with the HRTs (data not shown). Remarkably, HRT but not SPT for shrimp was positive in patient 9. This result shows that appropriately diluted food extracts can make the HRT a useful adjunct in the diagnosis of FDEIA. Also, specific IgE antibodies against ω-5-gliadin were detected in all of the five patients with FDEIA in this study in whom wheat was the culprit, confirming the importance of specific IgE antibodies against ω-5-gliadin in the diagnosis of wheat-induced FDEIA (WDEIA) (24).

Triggering factors for FDEIA are varied and include causative foods, exercise intensity (12), general fatigue, alcohol ingestion, cold temperature, the menstrual cycle, and aspirin (9, 10, 13, 16, 25–27). the mechanism responsible for the symptoms of FDEIA remains unclear. Concerning the role of exercise, it has been reported that increased blood levels of gliadin correlate with clinical symptoms induced by exercise in patients with WDEIA (16, 19).

Leakage from the gastrointestinal tract into the circulation was strongly induced by acute exercise in mice sensitized with gliadin and glutenin as allergens (28). Among the triggering factors, aspirin intake, especially, has been investigated in depth and reported regarding its role in provoking severe symptoms or in aggravating the symptoms of FDEIA (9, 10, 15).

Two possible mechanisms for the aspirin-induced symptoms in patients with FDEIA have been documented: up-regulation of antigen absorption across the intestinal epithelium and activation of mast cells (14–16). The latter possibility is supported by only a single previous report that SPTs with a causative food allergen were enhanced by pretreatment with oral aspirin in 5 of 8 patients with FDEIA (15). In our study, skin tests with the causative food allergen were stabilized by pretreatment with aspirin in 5 of the 7 patients tested. HRT with the causative food allergen did not increase significantly after aspirin intake in 8 of the 9 patients.

In summary, *in vivo* SPTs and *in vitro* HRTs did not show significant differences before or after aspirin intake in most of the patients with FDEIA, suggesting that the main mechanism for exacerbation of FDEIA symptoms by aspirin intake is independent of the acceleration of histamine release from mast cells/basophils. These data may support the hypothesis that antigen absorption plays a major role in the aspirin-induced aggravation of symptoms in FDEIA.

ACKNOWLEDGEMENTS

This work was supported in part by a Grant-in-Aid for Young Scientists (B) from the Ministry of Education, Culture, Sports, Science, and Technology, Japan (to A. Fukunaga).

REFERENCES

1. Sheffer AL, Austen KF. Exercise-induced anaphylaxis. J Allergy Clin Immunol 1980; 66: 106–111.
2. Maulitz RM, Pratt DS, Schocket AL. Exercise-induced anaphylactic reaction to shellfish. J Allergy Clin Immunol 1979; 63: 433–434.
3. Kushimoto H, Aoki T. Masked type I wheat allergy. Relation to exercise-induced anaphylaxis. Arch Dermatol 1985; 121: 355–360.
4. Kidd JM, 3rd, Cohen SH, Sosman AJ, Fink JN. Food-dependent exercise-induced anaphylaxis. J Allergy Clin Immunol 1983; 71: 407–411.
5. Fukunaga A, Bito T, Tsuru K, Oohashi A, Yu X, Ichihashi M, et al. Responsiveness to autologous sweat and serum in cholinergic urticaria classifies its clinical subtypes. J Allergy Clin Immunol 2005; 116: 397–402.
6. Horikawa T, Fukunaga A, Nishigori C. New concepts of hive formation in cholinergic urticaria. Curr Allergy Asthma Rep 2009; 9: 273–279.
7. Romano A, Di Fonso M, Giuffreda F, Quaratino D, Papa G, Palmieri V, et al. Diagnostic work-up for food-dependent, exercise-induced anaphylaxis. Allergy 1995; 50: 817–824.
8. Romano A, Di Fonso M, Giuffreda F, Papa G, Artesani MC, Viola M, et al. Food-dependent exercise-induced anaphylaxis: clinical and laboratory findings in 54 subjects. Int Arch Allergy Immunol 2001; 125: 264–272.
9. Dohi M, Suko M, Sugiyama H, Yamashita N, Tadokoro K, Juji F, et al. Food-dependent, exercise-induced anaphylaxis: a study on 11 Japanese cases. J Allergy Clin Immunol 1991; 87: 34–40.
10. Harada S, Horikawa T, Ashida M, Kamo T, Nishioka E, Ichihashi M. Aspirin enhances the induction of type I allergic symptoms when combined with food and exercise in patients with food-dependent exercise-induced anaphylaxis. Br J Dermatol 2001; 145: 336–339.
11. Harada S, Horikawa T, Icihashi M. [A study of food-dependent exercise-induced anaphylaxis by analyzing the Japanese cases reported in the literature]. Arerugi 2000; 49: 1066–1073 (in Japanese).
12. Loibl M, Schwarz S, Ring J, Halle M, Brockow K. Definition of an exercise intensity threshold in a challenge test to diagnose food-dependent exercise-induced anaphylaxis. Allergy 2009; 64: 1560–1561.
13. Bito T, Kanda E, Tanaka M, Fukunaga A, Horikawa T, Nishigori C. Cows milk-dependent exercise-induced anaphylaxis under the condition of a premenstrual or ovulatory phase following skin sensitization. Allergol Int 2008; 57: 437–439.
14. Morita E, Kunie K, Matsuo H. Food-dependent exercise-induced anaphylaxis. J Dermatol Sci 2007; 47: 109–117.
15. Aihara M, Miyazawa M, Osuna H, Tsubaki K, Ikebe T, Aihara Y, et al. Food-dependent exercise-induced anaphylaxis: influence of concurrent aspirin administration on skin testing and provocation. Br J Dermatol 2002; 146: 466–472.
16. Matsuo H, Morimoto K, Akaki T, Kaneko S, Kusatake K, Kuroda T, et al. Exercise and aspirin increase levels of circulating gliadin peptides in patients with wheat-dependent exercise-induced anaphylaxis. Clin Exp Allergy 2005; 35: 461–466.
17. Wojnar RJ, Hearn T, Starkweather S. Augmentation of allergic histamine release from human leukocytes by non-steroidal anti-inflammatory-analgesic agents. J Allergy Clin Immunol 1980; 66: 37–45.
18. Marone G, Kagey-Sobotka A, Lichtenstein LM. Effects of arachidonic acid and its metabolites on antigen-induced histamine release from human basophils in vitro. J Immunol 1979; 123: 1669–1677.
19. Takahashi A, Nakajima K, Ikeda M, Sano S, Kohno K, Morita E. Pre-treatment with misoprostol prevents food-dependent exercise-induced anaphylaxis (FDEIA). Int J Dermatol 2011; 50: 237–238.
20. Bruce RA, Blackmon JR, Jones JW, Strait G. Exercising testing in adult normal subjects and cardiac patients. 1963. Ann Noninvasive Electrocardiol 2004; 9: 291–303.
21. Takemoto H, Nishimura S, Kosada Y, Hata S, Takagi S, Hosoi S, et al. Anti-human IgE monoclonal antibodies recognizing epitopes related to the binding sites of high and low affinity IgE receptors. Microbiol Immunol 1994; 38: 63–71.
22. Fukunaga A, Hatakeyama M, Taguchi K, Shimizu H, Horikawa T, Nishigori C. Aspirin-intolerant chronic urticaria exacerbated by cutaneous application of a ketoprofen poultice. Acta Derm Venereol 2010; 90: 413–415.
23. Barg W, Wolanczyk-Medrala A, Obojski A, Wytrychowski K, Panaszek B, Medrala W. Food-dependent exercise-induced anaphylaxis: possible impact of increased basophil histamine releasability in hyperosmolar conditions. J Investig Allergol Clin Immunol 2008; 18: 312–315.
24. Morita E, Matsuo H, Chinuki Y, Takahashi H, Dahlstrom J, Tanaka A. Food-dependent exercise-induced anaphylaxis – importance of omega-5 gliadin and HMW-glutenin as causative antigens for wheat-dependent exercise-induced anaphylaxis. Allergol Int 2009; 58: 493–498.
25. Hanakawa Y, Tohyama M, Shirakata Y, Murakami S, Hashimoto K. Food-dependent exercise-induced anaphylaxis: a case related to the amount of food allergen ingested. Br J Dermatol 1998; 138: 898–900.
26. Aihara Y, Kotoyori T, Takahashi Y, Osuna H, Ohnuma S, Ikezawa Z. The necessity for dual food intake to provoke food-dependent exercise-induced anaphylaxis (FEIAn): a case report of FEIAn with simultaneous intake of wheat and umeboshi. J Allergy Clin Immunol 2001; 107: 1100–1105.
27. Shimizu T, Furumoto H, Kinoshita E, Ogasawara Y, Nakamura C, Hashimoto Y, et al. Food-dependent exercise-induced anaphylaxis occurring only in winter. Dermatology 2000; 200: 279.
28. Kozai H, Yano H, Matsuda T, Kato Y. Wheat-dependent exercise-induced anaphylaxis in mice is caused by gliadin and glutenin treatments. Immunol Lett 2006; 102: 83–90.

JAPANESE DERMATOLOGICAL ASSOCIATION
THE JOURNAL OF DERMATOLOGY
Journal of Dermatology 2012; **39**: 555–586

LETTERS TO THE EDITOR

Drug fever due to S-carboxymethyl-L-cystein: Demonstration of a causative agent with patch tests

Dear Editor,

Drug fever is a febrile response to a drug without skin manifestations and happens temporally following administration of the causative drug and disappears after discontinuation of the drug.[1] The most frequent mechanism of drug fever is a hypersensitivity reaction. However, its exact pathogenesis remains poorly understood.[2] S-carboxymethyl-L-cystein (SCMC) has been used worldwide for many years as an expectorant to treat chronic obstructive airway disease and bronchitis, and reported adverse reactions to that agent are rare.[3] Here, we report a first case of drug fever caused by SCMC.

A 67-year-old woman developed a fever of 39.5°C without any eruptions after an intake of SCMC and dextromethorphan hydrobromide hydrate and after an administration of SCMC and clarithromycin in August 2009 as cold medicine. Physical examinations causing a fever and laboratory tests revealed no abnormalities. She also had experienced an episode of febrile response after taking SCMC in 2002. After stopping an administration of drugs including SCMC, these episodes of febrile responses disappeared. These clinical histories suggested the possible diagnosis of drug fever due to SCMC. It was considered that the recurrence of fever after rechallenge with the suspected drug strengthens the definitive diagnosis of drug fever but the risks and benefits of rechallenge should be weighed.[1,2] Because the patient wanted an exact diagnosis and a cause of episodic fever, rechallenge with the suspected drug was performed in the hospital after obtaining informed consent. Fifty milligrams of SCMC (1/10th the normal dose) was administrated at 13.00 and 19.00 hours and on the following day 500 mg SCMC was further administrated at 09.00 and 13.00 hours, resulting in no fervescence. However, the administration of 500 mg SCMC at 20.00 hours induced a definite fever of 37.4°C 5–12-h later with an "inappropriately well" condition but without any eruptions (Fig. 1). An increase in C-reactive protein (4.05 mg/dL) occurred the following day after the intake of 500 mg SCMC at night. Due to these examinations, this patient was diagnosed as having drug fever due to SCMC.

Because administration of SCMC at night but not in the daytime induced fever and thiodiglycolic acid (TDA), its night-time metabolite, was suggested to be the causative agent of fixed drug eruptions induced by SCMC,[4,5] we hypothesized that this time-dependent febrile reaction induced by SCMC was due to its night-time metabolism. Because a common mechanism for the development of drug fever is thought to be a T-cell-mediated hypersensitivity reaction,[1,2] patch tests using SCMC and its metabolites (S-methyl-L-cystein [SMC] and TDA [Sigma-Aldrich, St Louis, MO, USA]) were performed to confirm the causative agent.[5] A patch test with 10% concentration of TDA was positive at day 2 and day 3 but 10% SCMC itself or SMC was not according to the International Contact Dermatitis Research Group criteria (Fig. 2).

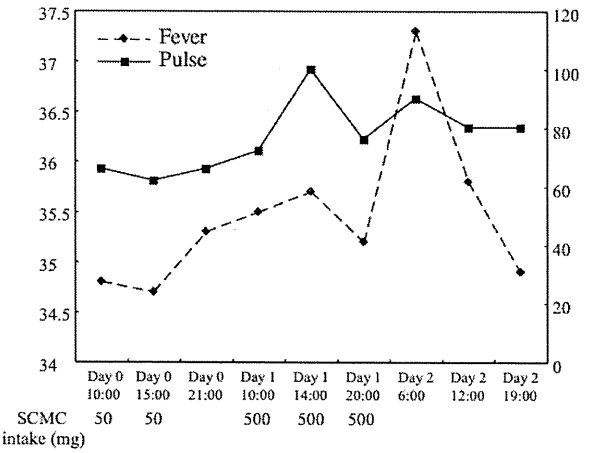

Figure 1. A febrile reaction during a rechallenge test with S-carboxymethyl-L-cystein (SCMC). Administration of SCMC at night but not in the daytime induced a febrile reaction.

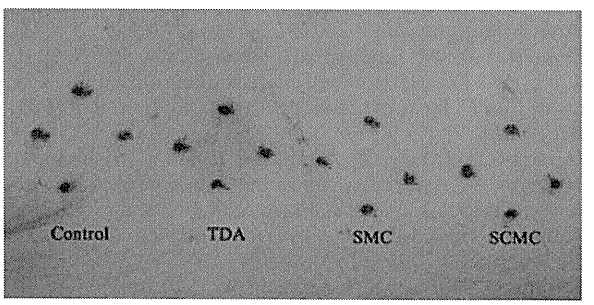

Figure 2. A patch test with 10% thiodiglycolic acid (TDA) was positive at day 2, but was negative for 10% S-carboxymethyl-L-cystein (SCMC) and for 10% S-methyl-L-cystein (SMC).

Five healthy volunteers had no positive reactions at those concentrations to the three chemicals.[4] Taken together, these data strongly suggest that TDA is the probable causative agent that induces drug fever due to SCMC in this patient.

The diagnosis of drug fever is often difficult and a careful review of a patient's clinical presentation as well as the drug history can lead to an exact diagnosis. In this patient, the exact diagnosis of drug fever due to SCMC could be made by a rechallenge test. No case of drug fever due to the widely-used SCMC has been reported so far. An administration of SCMC at night but not in the daytime

Correspondence: Atsushi Fukunaga, M.D., Division of Dermatology, Department of Internal Related, Kobe University Graduate School of Medicine, 7-5-1 Kusunoki-cho, Chuo-ku, Kobe 650-0017, Japan. Email: atsushi@med.kobe-u.ac.jp

induced a febrile reaction. This time-dependent febrile reaction led us to hypothesize that the causative agent is a night-time metabolite of SCMC but not SCMC itself. Consequently, patch testing with metabolites of SCMC revealed that the night-time metabolite TDA is the probable causative agent of the drug fever of this patient. Because SCMC is mainly metabolized via sulfoxidation, in a condition of lesser sulfoxidation ability due to a time-dependent reason (night-time) or genetic background, a different metabolite such as TDA is produced. Consequently, following night-time administration of SCMC, more of the parent compound is allowed to be converted to TDA and such a metabolic switching causes increase in TDA production.[3] Because these SCMC sulfoxidation capacities are thought to be under genetic control, the sulfoxidation ability in this patient and patients with drug eruptions caused by SCMC could be determined in future. Even in cases without skin eruption, patch tests may be beneficial for certain patients with drug fever that is caused by a hypersensitivity reaction. Because the cause of drug fever can be metabolites of a drug but not the drug itself, metabolites should be carefully considered when investigating the causative agent of drug fever.

Mayumi HATAKEYAMA,[1] Atsushi FUKUNAGA,[1]
Hideki SHIMIZU,[1] Masahiro OKA,[1]
Tatsuya HORIKAWA,[2] Chikako NISHIGORI[1]
[1]*Division of Dermatology, Department of Internal Related, Kobe University Graduate School of Medicine, and* [2]*Department of Dermatology, Nishi-Kobe Medical Center, Kobe, Japan*

REFERENCES

1 Patel RA, Gallagher JC. Drug fever. *Pharmacotherapy* 2010; **30**: 57–69.
2 Johnson DH, Cunha BA. Drug fever. *Infect Dis Clin North Am* 1996; **10**: 85–91.
3 Steventon GB, Mitchell SC. Thiodiglycolic acid and dermatological reactions following S-carboxymethyl-L-cysteine administration. *Br J Dermatol* 2006; **154**: 386–387.
4 Adachi A, Sarayama Y, Shimizu H *et al.* Thiodiglycolic acid as a possible causative agent of fixed drug eruption provoked only after continuous administration of S-carboxymethyl-L-cysteine: case report and review of reported cases. *Br J Dermatol* 2005; **153**: 226–228.
5 Steventon GB. Diurnal variation in the metabolism of S-carboxymethyl-L-cysteine in humans. *Drug Metab Dispos* 1999; **27**: 1092–1097.

Novel clinical and molecular findings in Chinese families with dyschromatosis symmetrica hereditaria

Dear Editor,

Dyschromatosis symmetrica hereditaria (DSH, Mendelian Inheritance in Man no. 127400) is a pigmentary genodermatosis characterized by a mixture of hyperpigmented and hypopigmented macules distributed on the back of the extremities. It is caused by mutation in the double-stranded RNA-specific adenosine deaminase (*DSRAD*) gene, which is also called the *ADAR1* gene encoding RNA-specific adenosine deaminase.[1] We describe an unusual case of concomitant DSH and psoriasis and an interesting case of DSH associated with depression. We performed direct nucleotide sequencing of the *DSRAD* gene in three Chinese families with DSH.

Our first case was a 32-year-old man with typical lesions of DSH on the back of his hands, but not on his feet. The patient reported erythematous, scaly papules and plaques appeared on his limbs and trunk 4 years previously (Fig. 1a,b). The biopsy specimen taken from the erythematous and scaly papules demonstrated parakeratosis with no granular layer, thickened epidermal papilla and dilated capillaries in the papillary dermis (Fig. 1c). These pathological findings were consistent with psoriasis. On the basis of clinical and histological findings, concomitant DSH and psoriasis were diagnosed. Our second case was a 52-year-old woman with typical lesions of DSH on the extremities. She reported that she felt isolated and worried of the lesions being seen by others because of the unpleasant appearance. When she was 18-years-old, she developed serious depression and wanted to commit suicide because of worrying that her marriage was being affected by the unpleasant appearance.

We performed a study of three families with DSH, including these two families. The study was approved by the Ethics Committee of Tianjin Medical University and informed consent was obtained from all participants. Genomic DNA was extracted (Tianamp Blood DNA Kit; Tiangen, Beijing, China) from whole blood samples of the patients, healthy family members and 100 unrelated controls. All translated exons and exon–intron boundaries sequences of the *DSRAD* gene were amplified by polymerase chain reaction (PCR). The amplified products were purified (High Pure PCR Product Purification Kit; Roche Applied Science, Mannheim, Germany) and sequenced using dye terminator chemistry on an automated DNA sequencer.

We identified three novel heterozygous mutations in the *ADAR1* gene as follows: (i) 1470 T→A (Fig. 2a) causing the nonsense mutation p.C490X in exon 2 identified in the patient with concomitant DSH and psoriasis; (ii) 1156 A→G (Fig. 2b) causing the missense mutation p.N386D in exon 2 identified in the patient with DSH and associated depression; and (iii) 3483 T→A (Fig. 2c) causing missense mutation p.I1161M in exon 15. The same mutations were not found in the healthy members of the families and the 100 unrelated normal controls, suggesting that they were not the common polymorphisms. None of the mutations in our patients have been previously reported.

Correspondence: Quanzhong Liu, M.D., Ph.D., Department of Dermatology, Tianjin Medical University General Hospital, 154 Anshan Dao, Tianjin 300052, China. Email: quanzhongliu2008@163.com

Departments of Dermatology[a] and Neurology,[b] University of Alabama at Birmingham; and Birmingham Veterans Affairs Medical Center[c]

Funding sources: None.

Conflicts of interest: None declared.

Correspondence to: Lauren C. Hughey, MD, Department of Dermatology, University of Alabama at Birmingham, 1530 Third Ave S, EFH 414, Birmingham, AL 35294

E-mail: lchughey@uab.edu

REFERENCES

1. Newsom-Davis J, Leys K, Vincent A, Ferguson I, Modi G, Mills K. Immunological evidence for the co-existence of the Lambert-Eaton myasthenic syndrome and myasthenia gravis in two patients. J Neurol Neurosurg Psychiatry 1991;54: 452-3.
2. Oh SJ, Sher E. MG and LEMS overlap syndrome: case report with electrophysiological and immunological evidence. Clin Neurophysiol 2005;116:1167-71.
3. Hamaguchi Y, Kuwana M, Hoshino K, Hasegawa M, Kaji K, Matsushita T, et al. Clinical correlations with dermatomyositis-specific autoantibodies in adult Japanese patients with dermatomyositis. Arch Dermatol 2011;147:391-8.
4. Hill C, Zhang Y, Sigurgeirsson B, Pukkala E, Mellemkjaer L, Airio A, et al. Frequency of specific cancer types in dermatomyositis and polymyositis: a population-based study. Lancet 2001; 357:96-100.
5. Leandro MJ, Isenberg DA. Rheumatic diseases and malignancy—is there an association? Scand J Rheumatol 2001;30: 185-8.
6. Leger JM, Bachoud-Levi AC, Eymard B, Theodore C, Bouche P, Pierrot-Deseilligny C. Paraneoplastic myasthenic syndrome. Rev Neurol (Paris) 1993;149:485-8.

doi:10.1016/j.jaad.2011.07.028

Detection of Merkel cell polyomavirus in cutaneous squamous cell carcinoma before occurrence of Merkel cell carcinoma

To the Editor: In 2008, a previously unknown polyomavirus, Merkel cell polyomavirus (MCPyV), was identified in Merkel cell carcinoma (MCC) lesions and close association between MCPyV and MCC has been suggested.[1,2] However, to our knowledge, no previous reports have confirmed MCPyV infection in patients with MCC before the occurrence of MCC. We herein report a patient who developed squamous cell carcinoma (SCC) followed by MCC. MCPyV was detected in both tumors by polymerase chain reaction analysis.

A 78-year-old Japanese man who had been immunosuppressed as a result of diabetes mellitus noticed a nodule on his right cheek, and the tumor was simply resected (Fig 1, *A*). The tumor was diagnosed histopathologically as typical SCC. Coexisting MCC was not found anywhere in the resected specimen by either hematoxylin-eosin stain or immunostaining for cytokeratin 20. One year later, he presented with a subcutaneous nodule in his left axillary lymph node. Positron emission computed tomography showed a solid mass (Fig 1, *B*). Histopathological, immunohistochemical, and ultrastructural examination revealed that the tumor was a nodal MCC, although the primary lesion was not discovered. Fourteen months after the axillary dissection, he developed multiple metastatic MCC lesions and died 10 months later.

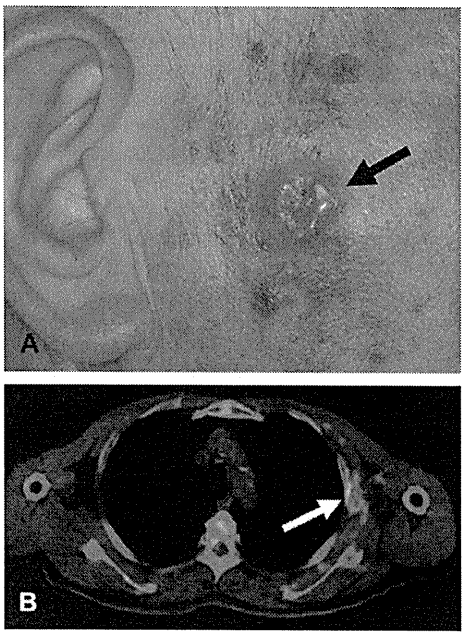

Fig 1. Squamous cell carcinoma (SCC) on right cheek (**A**) and Merkel cell carcinoma (MCC) in left axilla (**B**). **A**, Patient presented with crater-shaped nodule on right cheek (*arrow*). Resected tumor was typical, moderately differentiated SCC. **B**, Positron emission computed tomography showed solid mass 10 × 30 mm in size in left axilla (*white arrow*). Histopathologically, lesion was diagnosed as nodal MCC.

The VP1 region of MCPyV DNA was amplified from DNA samples both of the MCC and the SCC lesions (Fig 2, *A*). Copy numbers of MCPyV DNA large tumor (LT) domain were determined by quantitative real-time polymerase chain reaction using the β-globin gene as an internal control. The MCPyV-LT/β-actin in the MCC sample was $3.9 \times 10^4/4.8 \times 10^5$ ($=8.1 \times 10^{-2}$ copies per cell), and that in the SCC sample was $8.1 \times 10^2/2.0 \times 10^3$ ($=4.0 \times 10^{-3}$ copies per cell). Larger copy numbers of viral genome were obtained in the MCC lesion. Immunohistochemical staining demonstrated that the MCC cells were

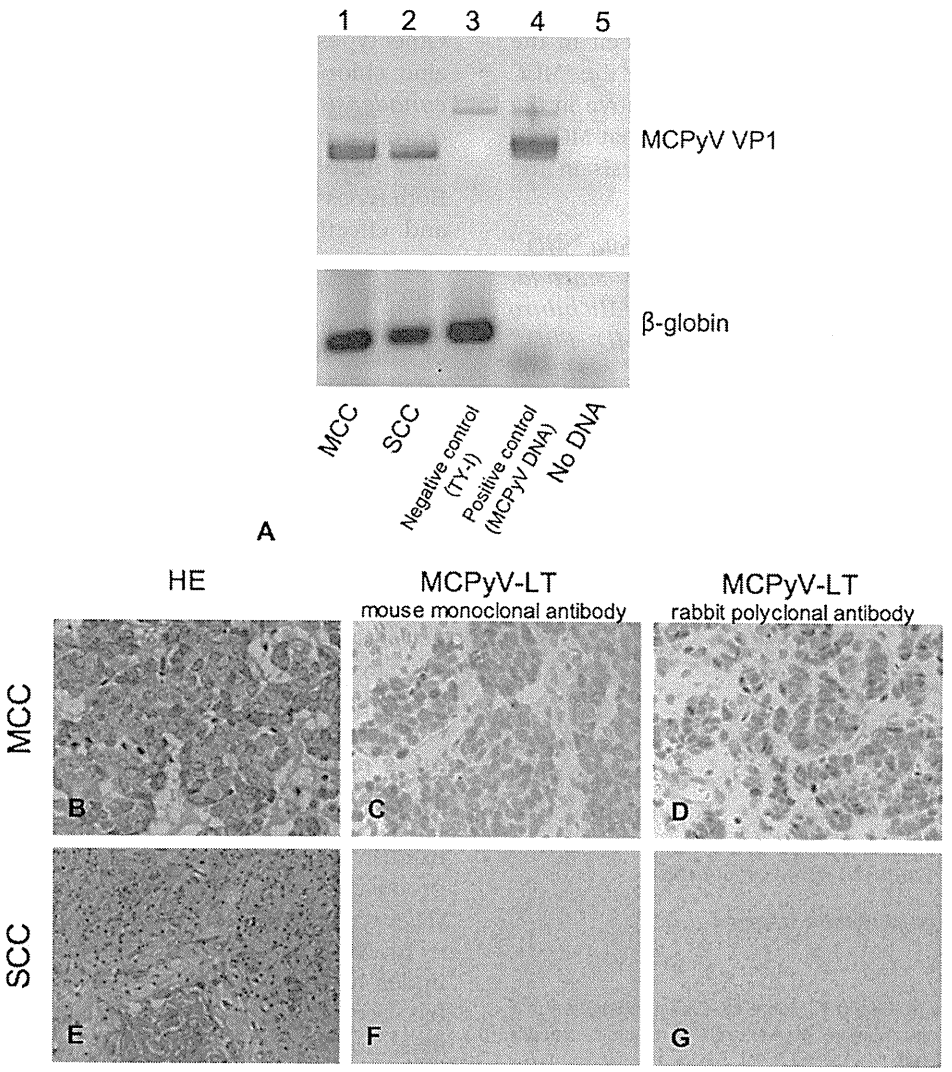

Fig 2. **A**, Detection of Merkel cell polyomavirus (*MCPyV*) by Southern blotting in polymerase chain reaction (PCR) products derived from Merkel cell carcinoma (*MCC*) and squamous cell carcinoma (*SCC*) lesions. Fragments of MCPyV were amplified by nested PCR from MCC lesions (lane 1) and SCC lesions (lane 2). Lower panel shows internal control PCR products of β-globin gene. **B** to **G**, Immunohistochemical detection of MCPyV-large tumor (*LT*) antigen in MCC and SCC lesions. Immunolabeling with mouse monoclonal antibody CM2B4 (**C**) and rabbit polyclonal antibody (**D**) detect LT antigen expression in diffuse nuclear pattern in tumor cells of MCC lesion. (Original magnification: ×400.) In contrast, tumor cells in SCC lesion show no MCPyV-LT antigen expression with CM2B4 (**F**) and rabbit polyclonal antibody (**G**) staining. (Original magnifications: ×400.) (**B** and **E**, Hematoxylin-eosin [*HE*] stain; original magnifications: ×400.)

positive for MCPyV-LT antigen, although the SCC cells were negative for it (Fig 2, *B* to *G*).

LT antigen is one of the tumor antigens encoded by MCPyV DNA. MCC cells frequently express this LT antigen in the nuclei.[3] Reisinger et al[4] reported that LT antigen was detected in 92% of MCC tumors from patients with secondary SCC or basal cell carcinoma. However, all the secondary non-MCC tumors were negative for LT antigen. Also in our case, LT antigen was positive only in the MCC, but negative in the SCC. On the other hand, our study revealed that MCPyV DNA was detected in SCC lesions that occurred before the MCC. Our results clearly indicate that the patient was infected with MCPyV at least 1 year before the occurrence of MCC, further attesting to the pathogenic role of MCPyV infection in MCC, although MCPyV has been found on the skin of

multiple healthy individuals with positive serologies.[5] The MCPyV copy number per cell in the SCC lesion was smaller than that in the MCC lesion. In addition, LT antigen was negative in the SCC lesion. Thus, we cannot conclude that MCPyV played a certain role in SCC oncogenesis in the current patient.

Kana Kaibuchi-Noda, MD,[a] Kenji Yokota, MD,[a] Takaaki Matsumoto, MD,[a] Masaki Sawada, MD,[a] Akihiro Sakakibara, MD, PhD,[a] Michihiro Kono, MD, PhD,[a] Yasushi Tomita, MD, PhD,[a] Daisuke Watanabe, MD, PhD,[b] Hitomi Fukumoto, MD,[c] Harutaka Katano, DDS, PhD,[c] and Masashi Akiyama, MD, PhD[a]

Department of Dermatology, Nagoya University Graduate School of Medicine[a]; Department of Dermatology, Aichi Medical University, Nagakute[b]; and Department of Pathology, National Institute of Infectious Diseases, Shinjuku, Tokyo[c]; Japan

Funding sources: None.

Conflicts of interest: None declared.

Correspondence to: Masashi Akiyama, MD, PhD, Department of Dermatology, Nagoya University Graduate School of Medicine, 65 Tsurumai-cho, Showa-ku, Nagoya, 466-8550 Japan

E-mail: makiyama@med.nagoya-u.ac.jp

REFERENCES

1. Feng H, Shuda M, Chang Y, Moore PS. Clonal integration of a polyomavirus in human Merkel cell carcinoma. Science 2008;319:1096-100.
2. Kassem A, Schöpfin A, Diaz C, Weyers W, Stickeler E, Werner M, et al. A frequent detection of Merkel cell polyomavirus in human Merkel cell carcinoma and identification of a unique deletion in the VP1 gene. Cancer Res 2008;68:5009-13.
3. Houben R, Shuda M, Weinkam R, Schrama D, Feng H, Chang Y, et al. Merkel cell polyomavirus-infected Merkel cell carcinoma cells require expression of viral T antigen. J Virol 2010;84: 7064-72.
4. Reisinger DM, Shiffer JD, Cognetta AB, Chang Y, Moore PS. Lack of evidence for basal or squamous cell carcinoma infection with Merkel cell polyomavirus in immunocompetent patients with Merkel cell carcinoma. J Am Acad Dermatol 2010;63:400-3.
5. Schowalter RM, Pastrana DV, Pumphrey KA, Moyer AL, Buck CB. Merkel cell polyomavirus and two previously unknown polyomaviruses are chronically shed from human skin. Cell Host Microbe 2010;7:509-15.

doi:10.1016/j.jaad.2011.06.026

Buyer beware: A black salve caution

To the Editor: Black salve ointments containing beeswax, cocoa butter, oil, charcoal, and clay have been used by the general public to treat boils, abscesses, bee stings, and other minor wounds. Other types of black salve products may also include zinc chloride or bloodroot extract (*Sanguinaria canadensis*), resulting in a biologically nonspecific corrosive escharotic agent capable of indiscriminately dissolving healthy and diseased tissue alike. Both types of products are advertised online as safe and effective for the treatment of more serious conditions, such as skin cancer, moles, warts, and skin tags. There are numerous testimonials online, but there are no scientific studies for clinical efficacy or safety. In addition, the wide diversity of poorly regulated black salve products, which often contain different ingredients and lack quality control, leads to confusion about the use of these products. We present a case that illustrates the danger of using poorly regulated online products perceived as safe and effective by the general public to treat serious dermatologic conditions.

A 63-year-old man had a history of an unknown neoplasm on his left naris. The neoplasm originally appeared in 1999 and, suspecting it to be a melanoma, he declined a biopsy and allopathic treatment, choosing rather to self-treat it with corrosive black salve product containing 300 mg of bloodroot, galangal, red clover, and sheep sorrel. After many months of treatment, the lesion resolved, however, extensive tissue damage imposed by the black salve product left the patient with an absent left naris (Figs 1 and 2).

In 2010, he returned with a hard, waxy nodule under his right eye. Biopsy specimen revealed a basal cell carcinoma. Despite his previous experience, the patient preferred to self-treat the lesion with the black salve product rather than have Mohs micrographic surgery. After a 4-month delay with no improvement, the patient reconsidered and consented to Mohs micrographic surgery. We could not determine if he would have had further recurrences, as a few months later, he was diagnosed with colon cancer and elected to self-treat this with oral black salve product and subsequently died.

The use of this black salve product resulted in severe skin damage. Histologic examination of tissues exposed to corrosive black salve products has shown extensive tissue necrosis with secondary necrotizing vasculitis.[1] Because of its escharotic character, corrosive black salve products may destroy both cancerous and healthy skin to a degree that eradicates the local cancer, but leaves an esthetically unpleasing result.[2] In addition, without a biopsy, there can be no guarantee the cancer has been completely eliminated. If residual cancer cells persist, the risk of recurrence and/or metastasis remains.[3,4] Self-treatment with black salve products

DOI:10.1111/j.1600-0625.2011.01384.x
www.blackwellpublishing.com/EXD

Letter to the Editor

Interleukin (IL)-17 versus IL-27: opposite effects on tumor necrosis factor-α-mediated chemokine production in human keratinocytes

Susumu Fujiwara[1], Hiroshi Nagai[1], Shuntaro Oniki[1], Takayuki Yoshimoto[2] and Chikako Nishigori[1]

[1]Division of Dermatology, Department of Internal Related, Kobe University Graduate School of Medicine, Kobe, Japan; [2]Intractable Disease Research Center, Tokyo Medical University, Tokyo, Japan

Correspondence: Hiroshi Nagai, Division of Dermatology, Department of Internal Related, Kobe University Graduate School of Medicine, 7-5-1 Kusunoki-cho, Chuo-ku, Kobe 650-0017, Japan, Tel.: +81 78 382 6134, Fax: +81 78 382 6149, e-mail: hnagai@med.kobe-u.ac.jp

Abstract: Tumor necrosis factor (TNF)-α is known to play a pivotal role in the pathogenesis of psoriasis. TNF-α has been shown to act directly on keratinocytes, thereby inducing the production of various kinds of chemokines, which contributes to the infiltration of leucocytes into the psoriatic lesions. Recent studies have shown that both interleukin (IL)-17 and IL-27 are increased in psoriatic lesional tissue. However, the interactions between TNF-α, IL-17 and IL-27 in chemokine production by keratinocytes have not been fully elucidated. Here, we examined in human keratinocytes how TNF-α, IL-17 and IL-27 affect production of chemokines that are involved in the pathogenesis of psoriasis. We found that IL-17 and IL-27 exert opposite effects on TNF-α-mediated chemokine production. This suggests that lesional balance of IL-17 and IL-27 is involved in the recruitment of T cells, natural killer cells, neutrophils, monocytes or dendritic cells, thereby affecting inflammation in skin diseases.

Abbreviations: Th, T helper.

Key words: chemokine – interleukin-17 – interleukin-27 – keratinocyte – tumor necrosis factor-α

Accepted for publication 29 September 2011

Background

It has been shown that various chemokines are involved in the pathogenesis of immune-mediated skin diseases. In psoriasis, CXCL10, CXCL8, CCL5, CCL20 and CCL2 are upregulated in lesional keratinocytes (1). Expression of CXCL8, CXCL10 and CCL20 in psoriatic lesions is markedly suppressed by treatment with tumor necrosis factor (TNF) blocker (2). Furthermore, psoriatic T cells and natural killer (NK) cells show maximal responses to CXCL10, CCL17 and CCL20, and to CXCL10 and CCL5, respectively (3). These results suggest that keratinocyte-derived chemokines play a crucial role in the pathogenesis of psoriasis.

Tumor necrosis factor-α is known to be increased and associated with many different inflammatory diseases (4,5). TNF-α acts on various cells via two receptors (TNFR1 and TNFR2), thereby inducing chemokine production, cell proliferation and apoptosis (6). It is well known that TNF-α plays a pivotal role in the pathogenesis of psoriasis (7). TNF-α acts directly on keratinocytes, thereby inducing production of various chemokines, which contribute to leucocyte infiltration into psoriatic lesions. Recent studies have shown that the amount of interleukin (IL)-17 is increased in psoriatic lesional tissue and decreased by effective treatment (8). Additionally, Shibata et al. (9) have reported that serum IL-27 levels in patients with psoriasis are significantly increased and that IL-27-secreting cells infiltrate the papillary dermis of lesions. Thus, both IL-17 and IL-27 are likely to play a role in psoriasis. Although IL-17 has previously been shown to upregulate TNF-α-induced CXCL8 and downregulate TNF-α-induced CCL5 in human keratinocytes (10), the interactions between TNF-α, IL-17 and IL-27 in chemokine production by keratinocytes have not been fully elucidated.

Questions addressed

This study aimed to clarify, in human keratinocytes, how TNF-α, IL-17 and IL-27 affect the production of chemokines involved in the pathogenesis of psoriasis, including CXCL1, CXCL2, CXCL8, CXCL9, CXCL10, CCL2, CCL5 and CCL20.

Experimental design

Normal human epidermal keratinocytes (NHEKs) from three different donors were purchased from Kurabo Industries Ltd. (Osaka, Japan). NHEKs (passage 2–4) were incubated with the recommended medium (Humedia-KG2; Kurabo) containing various combinations of IL-17 (50 ng/ml; Pepro Tech Inc., Rocky Hill, NJ, USA), IL-27 (10 or 100 ng/ml; R&D Systems Inc., Minneapolis, MN, USA) and TNF-α (10 ng/ml; Pepro Tech) for 24 h. For stimulation with combinations of multiple cytokines, the cytokines were added simultaneously. The levels of chemokines in the supernatants were determined by ELISA (CXCL1 and CXCL10, RayBiotech Inc., Norcross, GA, USA; CXCL2, Pepro Tech; CXCL8, CXCL9, CCL2, CCL5 and CCL20, R&D Systems). The experiments were conducted at least twice using each NHEK. Data were expressed as the mean ± SE of three samples and compared using analysis of variance (ANOVA), with *post hoc* testing using the Tukey–Kramer and Scheffe's methods.

Results

Analysis of the ELISA data revealed that many psoriasis-related chemokines were induced by TNF-α and that the chemokines could be categorized into two groups: those whose production could be enhanced by IL-17 independently or synergistically with TNF-α, and those whose production could be enhanced by IL-27 independently or synergistically with TNF-α. The former (hereafter referred to as the IL-17-enhancing group) included CXCL1,

Table 1. Chemokine release from keratinocytes stimulated with tumor necrosis factor (TNF)-α, interleukin (IL)-17 and IL-27 alone or in combination

Treatment[1]	CXCL1 (pg/ml)	CXCL2 (pg/ml)	CXCL8 (pg/ml)	CCL20 (pg/ml)
None				
NHEK1	2500 ± 121	372 ± 15	633 ± 8.4	59 ± 1.2
NHEK2	3210 ± 74	85 ± 3.7	39 ± 1.4	23 ± 0.66
NHEK3	2545 ± 75	363 ± 7.0	132 ± 2.1	83 ± 0.15
IL-17				
NHEK1	11269 ± 202[2]	438 ± 5.3[2]	1038 ± 63[2]	306 ± 5.7[2]
NHEK2	7039 ± 163[2]	111 ± 4.4[2]	148 ± 6.7[2]	92 ± 1.5[2]
NHEK3	10575 ± 1122[2]	469 ± 9.7[2]	417 ± 0.99[2]	477 ± 1.9[2]
IL-27 (10 ng/ml)				
NHEK1	2219 ± 27	333 ± 11	670 ± 73	56 ± 2.2
NHEK2	2648 ± 61	74 ± 4.3	48 ± 6.0	24 ± 0.073
NHEK3	2455 ± 4.8	342 ± 1.5	131 ± 6.9	80 ± 1.3
TNF-α				
NHEK1	6735 ± 24[2]	430 ± 14[2]	2151 ± 100[2]	409 ± 4.1[2]
NHEK2	7272 ± 143[2]	125 ± 2.9[2]	282 ± 5.7[2]	133 ± 4.0[2]
NHEK3	7415 ± 177[2]	457 ± 10[2]	543 ± 6.1[2]	345 ± 13[2]
IL-17 + IL-27 (10 ng/ml)				
NHEK1	9379 ± 212	382 ± 5.7	1137 ± 61	302 ± 0.43
NHEK2	6566 ± 107	90 ± 1.72	201 ± 11	89 ± 0.51
NHEK3	10734 ± 110	408 ± 6.4	418 ± 1.4	489 ± 9.3
TNF-α + IL-27 (10 ng/ml)				
NHEK1	5266 ± 58[3]	377 ± 8.4[3]	1873 ± 46[3]	372 ± 5.2[3]
NHEK2	6909 ± 53	99 ± 5.0[3]	191 ± 5.5[3]	138 ± 5.9
NHEK3	7081 ± 134	355 ± 15[3]	471 ± 16[3]	345 ± 1.5
TNF-α + IL-27 (100 ng/ml)				
NHEK1	5060 ± 60[3]	382 ± 8.2	2064 ± 116	410 ± 13
NHEK2	5096 ± 118[3]	99 ± 3.5[3]	225 ± 5.6[3]	100 ± 2.6[3]
NHEK3	6186 ± 334[3]	306 ± 4.5[3]	521 ± 15	300 ± 2.6[3]

Treatment[1]	CXCL9 (pg/ml)	CXCL10 (pg/ml)	CCL2 (pg/ml)	CCL5 (pg/ml)
None				
NHEK1	0.00 ± 0.00	116 ± 37	3.4 ± 0.74	11 ± 0.13
NHEK2	0.63 ± 0.00	27 ± 8.6	30 ± 0.26	0.22 ± 0.16
NHEK3	21 ± 3.7	10 ± 0.32	24 ± 0.79	2.2 ± 0.16
IL-17				
NHEK1	8.6 ± 3.3	133 ± 23	6.0 ± 0.80	9.4 ± 0.11
NHEK2	0.00 ± 0.00	15 ± 2.3	28 ± 0.26	0.21 ± 0.094
NHEK3	17 ± 8.7	13 ± 1.4	21 ± 0.80	0.88 ± 0.25
IL-27 (10 ng/ml)				
NHEK1	5306 ± 288[2]	214 ± 70	12.2 ± 0.00	13 ± 0.15
NHEK2	579 ± 36[2]	346 ± 113	29 ± 1.0	0.49 ± 0.052
NHEK3	37 ± 10	203 ± 50	31 ± 0.51	11 ± 0.33
TNF-α				
NHEK1	5.7 ± 2.2	883 ± 90	10 ± 0.84	91 ± 0.73[2]
NHEK2	0.00 ± 0.00	259 ± 26	49 ± 0.99	13 ± 0.33[2]
NHEK3	12 ± 5.8	90 ± 16	34 ± 1.0	42 ± 0.20[2]
IL-17 + IL-27 (10 ng/ml)				
NHEK1	6980 ± 622	897 ± 284	8.4 ± 1.1	11 ± 0.12
NHEK2	580 ± 8.9	32 ± 10	30 ± 0.00	0.35 ± 0.043
NHEK3	24 ± 3.5	13 ± 5.6	28 ± 0.78	4.1 ± 0.70
TNF-α + IL-17				
NHEK1	6.6 ± 2.5	436 ± 24	23 ± 0.53	68 ± 0.76[3]
NHEK2	0.59 ± 0.59	147 ± 7.9	45 ± 1.8	11 ± 0.70
NHEK3	13 ± 6.7	48 ± 8.3	36 ± 2.0	35 ± 1.4
TNF-α + IL-27 (10 ng/ml)				
NHEK1	27827 ± 359[3]	8781 ± 434	49 ± 0.98[3]	233 ± 2.56[3]
NHEK2	2159 ± 20[3]	4906 ± 242	47 ± 1.0	17 ± 1.2
NHEK3	99 ± 16[3]	995 ± 154	41 ± 0.74	117 ± 2.6[3]
TNF-α + IL-27 (100 ng/ml)				
NHEK1	35735 ± 461[3]	235278 ± 4486[3]	141 ± 3.6[3]	344 ± 4.1[3]
NHEK2	2772 ± 72[3]	131455 ± 2510[3]	303 ± 8.6[3]	100 ± 2.2[3]
NHEK3	127 ± 20[3]	49403 ± 1547[3]	269 ± 5.7[3]	306 ± 4.8[3]
TNF-α + IL-17 + IL-27 (10 ng/ml)				
NHEK1	16039 ± 1218[4]	3357 ± 273	41 ± 0.28	118 ± 1.9[4]
NHEK2	953 ± 23[4]	4633 ± 376	45 ± 0.96	13 ± 1.0
NHEK3	37 ± 7.8	53 ± 53	40 ± 0.28	53 ± 1.1[4]
TNF-α + IL-17 + IL-27 (100 ng/ml)				
NHEK1	20845 ± 1583[5]	66025 ± 6191[5]	72 ± 0.67[5]	157 ± 2.8[5]
NHEK2	1238 ± 15[5]	91119 ± 8545[5]	225 ± 6.9[5]	56 ± 0.72[5]
NHEK3	48 ± 10[5]	34244 ± 1072[5]	153 ± 1.3[5]	81 ± 1.1[5]

NHEK, normal human epidermal keratinocyte.
[1]NHEKs derived from three donors (NHEK1–3) were seeded in six-well plates (1.5×10^5 cells/well) in serum-free medium and treated with the indicated cytokines at the following concentrations: 50 ng/ml IL-17, 10 or 100 ng/ml IL-27, and 10 ng/ml TNF-α. Chemokine levels were measured by ELISA on supernatants collected after 24 h of stimulation.
[2]$P < 0.05$-$P < 0.001$; versus untreated cells.
[3]$P < 0.05$-$P < 0.001$; versus TNF-α-treated cells.
[4]$P < 0.05$-$P < 0.001$; versus TNF-α and IL-27 (10 ng/ml)-treated cells.
[5]$P < 0.05$-$P < 0.001$; versus TNF-α and IL-27 (100 ng/ml)-treated cells.

Table 2. Interleukin (IL)-17 and IL-27 exert opposite effect on the tumor necrosis factor (TNF)-α-mediated production of psoriasis-related chemokines in keratinocyte

	IL-17	IL-27
CXCL1	↑	↓[1]
CXCL2	↑	↓[1]
CXCL8	↑	↓[1]
CCL20	↑	↓[1]
CXCL9	↓[2]	↑[3]
CXCL10	↓[2]	↑[3]
CCL2	↓[2]	↑[3]
CCL5	↓[2]	↑[3]

↑: enhance; ↓: suppress.
[1]Suppression of the chemokine expression induced by TNF-α.
[2]Suppression of the chemokine expression synergistically induced by TNF-α and IL-27.
[3]Enhancement of the chemokine expression by IL-27 independently or synergistically with TNF-α.

CXCL2, CXCL8 and CCL20; the latter (the IL-27-enhancing group) included CXCL9, CXCL10, CCL2 and CCL5. IL-17 and IL-27 tended to suppress the TNF-α-mediated production of the IL-27- and IL-17-enhancing groups, respectively (Tables 1 and 2, Figures S1 and S2). Neither IL-17 nor IL-27 significantly affected the IL-27- and IL-17-induced production of chemokines, respectively.

Discussion

Recently, Lee et al. have shown that IL-17 represses TNF-α-stimulated expression of CXCL10 and CCL5, but acts synergistically with TNF-α for induction of CXCL1, CXCL8 and CCL20 in intestinal epithelial cells. They also have shown that IL-17 induces CXCL8 by stabilizing its mRNA and negatively regulates CXCL10 by repressing its transcription, and that both forms of regulation are dependent on the p38 and ERK MAPK signalling pathways (11). Although we suspect similar molecular events occur in keratinocytes, the mechanisms underlying the opposite effects of IL-17 and IL-27 are unknown. Interestingly, Wittmann et al. (12) have shown that CXCL10 is produced significantly more by keratinocytes when IL-27 precedes TNF-α than the other way around. This priming property for IL-27 with regard to TNF-α is noteworthy and seems to be relevant to the synergistic effects of IL-27 and TNF-α on the chemokine production of the IL-27-enhancing group, although the two cytokines were simultaneously added in our study.

Our results indicate the possibility that the balance of IL-17 and IL-27 may affect leucocyte infiltration in psoriatic lesions. According to the characteristics of chemokines, IL-17 may contribute to the recruitment of neutrophils, dendritic cells and T helper (Th)17 cells but inhibit that of Th1 cells, NK cells and monocytes into inflamed skin, whereas IL-27 might have the opposite effect. Recently, Th17 cells have been shown to play a role in the pathogenesis of atopic dermatitis (13). Furthermore, it has been reported that IL-27 is also expressed in chronic human eczematous lesions (12). Thus, both IL-17 and IL-27, along with TNF-α, are likely to be expressed also in eczematous lesions, where IL-17 and IL-27 may exert opposite effects on chemokine production. Interestingly, IL-17 and IL-27 have previously been demonstrated to have opposite effects on angiogenesis (pro- and antiangiogenic activity, respectively) (14,15). Additionally, IL-27 has been shown to limit Th17 activity or development (16). These

findings and our data imply that IL-17 and IL-27 may have opposite effects in various *in vivo* situations. The significance of our findings might be relevant to other systemic inflammatory diseases that involve TNF-α, including Crohn's disease and ulcerative colitis; both IL-17 and IL-27 are expressed in the affected mucosa, and many chemokines are suggested to be involved in the pathogenesis (17–19).

In conclusion, we found that IL-17 and IL-27 exert opposite effects on the TNF-α-mediated chemokine production in human keratinocytes. This result suggests that lesional levels of IL-17 and IL-27 may be involved in the recruitment of neutrophils, dendritic cells, monocytes, T cells or NK cells, thereby affecting inflammation in skin diseases. Although further studies using other cells are needed, the paired effects of these two cytokines might be relevant to other TNF-α-mediated inflammatory diseases.

Acknowledgements

Susumu Fujiwara performed the research; Susumu Fujiwara and Hiroshi Nagai analysed the data; Hiroshi Nagai, Shuntaro Oniki and Takayuki Yoshimoto designed the research study; and Hiroshi Nagai and Chikako Nishigori wrote the article. This work was in part supported by Grand-in Aid for Scientific Research (H.N.) and by the Support Programme for Improving Graduate School Education from the Ministry of Education, Culture, Sports, Science and Technology of Japan (S.F.).

Conflict of interests

The authors have no conflicts of interest to declare.

References

1 Giustizieri M L, Mascia F, Frezzolini A *et al.* J Allergy Clin Immunol 2001: **107**: 871–877.
2 Gottlieb A B, Chamian F, Masud S *et al.* J Immunol 2005: **175**: 2721–2729.
3 Ottaviani C, Nasorri F, Bedini C *et al.* Eur J Immunol 2006: **36**: 118–128.
4 Bradley J R. J Pathol 2008: **214**: 149–160.
5 Jurisic V, Terzic T, Colic S *et al.* Oral Dis 2008: **14**: 600–605.
6 Jurisic V, Bogdanovic G, Kojic V *et al.* Ann Hematol 2006: **85**: 86–94.
7 de Groot M, Teunissen M B, Picavet D I *et al.* Exp Dermatol 2010: **19**: 754–756.
8 Lowes M A, Kikuchi T, Fuentes-Duculan J *et al.* J Invest Dermatol 2008: **128**: 1207–1211.
9 Shibata S, Tada Y, Kanda N *et al.* J Invest Dermatol 2010: **130**: 1034–1039.
10 Albanesi C, Cavani A, Girolomni G. J Immunol 1999: **162**: 494–502.
11 Lee J W, Wang P, Kattah M G *et al.* J Immunol 2008: **181**: 6536–6545.
12 Wittmann M, Zeitvogel J, Wang D *et al.* J Allergy Clin Immunol 2009: **124**: 81–89.
13 Koga C, Kabashima K, Shiraishi N *et al.* J Invest Dermatol 2008: **128**: 2625–2630.
14 Numasaki M, Fukushi J, Ono M *et al.* Blood 2003: **101**: 2620–2627.
15 Shimizu M, Shimamura M, Owaki T *et al.* J Immunol 2006: **176**: 7317–7324.
16 Stumhofer J S, Laurence A, Wilson E H *et al.* Nat Immunol 2006: **7**: 937–945.
17 Sugihara T, Kobori A, Imaeda H *et al.* Clin Exp Immunol 2010: **160**: 386–393.
18 León A J, Gómez E, Garrote J A *et al.* Mediators Inflamm 2009: **2009**: 580450.
19 Nishimura M, Kuboi Y, Muramoto K *et al.* Ann N Y Acad Sci 2009: **1173**: 350–356.

Supporting information

Additional Supporting Information may be found in the online version of this article:

Figure S1. IL-27 suppresses TNF-α-induced production of the IL-17-enhancing group.

Figure S2. IL-17 suppresses production of the IL-27-enhancing group that was synergistically induced by TNF-α and IL-27.

Please note: Wiley-Blackwell is not responsible for the content or functionality of any supporting materials supplied by the authors. Any queries (other than missing material) should be directed to the corresponding author for the article.

DOI:10.1111/j.1600-0625.2011.01400.x
www.blackwellpublishing.com/EXD

Letter to the Editor

Bioactive reagents used in mesotherapy for skin rejuvenation *in vivo* induce diverse physiological processes in human skin fibroblasts *in vitro* – a pilot study

Claudia Jäger[1], Christiane Brenner[2], Jüri Habicht[2] and Reinhard Wallich[2]

[1]ATOS Clinic Heidelberg, Bismarckstr, Heidelberg, Germany; [2]Institute for Immunology, University Clinics Heidelberg, Heidelberg, Germany
Correspondence: Claudia Jäger, MD, ATOS Clinic Heidelberg, Bismarckstr. 9-15, D-69115 Heidelberg, Germany, Tel.: +49-6221-983345, Fax: +49-6221-864681, e-mail: claudia.jaeger@atos.de

Abstract: The promise of mesotherapy is maintenance and/or recovery of a youthful skin with a firm, bright and moisturized texture. Currently applied medications employ microinjections of hyaluronic acid, vitamins, minerals and amino acids into the superficial layer of the skin. However, the molecular and cellular processes underlying mesotherapy are still elusive. Here we analysed the effect of five distinct medication formulas on pivotal parameters involved in skin ageing, that is collagen expression, cell proliferation and morphological changes using normal human skin fibroblast cultures *in vitro*. Whereas in the presence of hyaluronic acid, NCTF135® and NCTF135HA®, cell proliferation was comparable to control cultures; however, with higher expression of collagen type-1, matrix metalloproteinase-1 and tissue inhibitor of matrix metalloproteinase-1, addition of Soluvit® N and Meso-BK led to apoptosis and/or necrosis of human fibroblasts. The data indicate that bioactive reagents currently applied for skin rejuvenation elicit strikingly divergent physiological processes in human skin fibroblast *in vitro*.

Key words: collagen type 1 – hyaluronic acid – mesotherapy – skin rejuvenation

Accepted for publication 20 October 2011

Dis Model Mech. 2011 November; 4(6): 777–785. PMCID: PMC3209647
Published online 2011 August 4. doi: 10.1242/dmm.007146

Abca12-mediated lipid transport and Snap29-dependent trafficking of lamellar granules are crucial for epidermal morphogenesis in a zebrafish model of ichthyosis

Qiaoli Li,[1,*] Michael Frank,[1,*] Masashi Akiyama,[2,3] Hiroshi Shimizu,[3] Shiu-Ying Ho,[4] Christine Thisse,[5] Bernard Thisse,[5] Eli Sprecher,[6] and Jouni Uitto[1,4,‡]

[1]Department of Dermatology and Cutaneous Biology, and
[4]Department of Biochemistry and Molecular Biology, Jefferson Medical College, Thomas Jefferson University, Philadelphia, PA 19107, USA
[2]Department of Dermatology, Nagoya University Graduate School of Medicine, Nagoya 466-8550, Japan
[3]Department of Dermatology, Hokkaido University Graduate School of Medicine, Sapporo 060-8638, Japan
[5]Department of Cell Biology, University of Virginia School of Medicine, Charlottesville, VA 22908, USA
[6]Department of Dermatology, Tel Aviv Medical Center, Tel Aviv 64239, Israel
*These authors equally contributed to this work
‡Author for correspondence (Email: Jouni.uitto@jefferson.edu)

Received October 29, 2010; Accepted May 27, 2011.

SUMMARY

Zebrafish (*Danio rerio*) can serve as a model system to study heritable skin diseases. The skin is rapidly developed during the first 5–6 days of embryonic growth, accompanied by expression of skin-specific genes. Transmission electron microscopy (TEM) of wild-type zebrafish at day 5 reveals a two-cell-layer epidermis separated from the underlying collagenous stroma by a basement membrane with fully developed hemidesmosomes. Scanning electron microscopy (SEM) reveals an ordered surface contour of keratinocytes with discrete microridges. To gain insight into epidermal morphogenesis, we have employed morpholino-mediated knockdown of the *abca12* and *snap29* genes, which are crucial for secretion of lipids and intracellular trafficking of lamellar granules, respectively. Morpholinos, when placed on exon-intron junctions, were >90% effective in preventing the corresponding gene expression when injected into one- to four-cell-stage embryos. By day 3, TEM of *abca12* morphants showed accumulation of lipid-containing electron-dense lamellar granules, whereas *snap29* morphants showed the presence of apparently empty vesicles in the epidermis. Evaluation of epidermal morphogenesis by SEM revealed similar perturbations in both cases in the microridge architecture and the development of spicule-like protrusions on the surface of keratinocytes. These morphological findings are akin to epidermal changes in harlequin ichthyosis and CEDNIK syndrome, autosomal recessive keratinization disorders due to mutations in the *ABCA12* and *SNAP29* genes, respectively. The results indicate that interference of independent pathways involving lipid transport in the epidermis can result in phenotypically similar perturbations in epidermal morphogenesis, and that these fish mutants can serve as a model to study the pathomechanisms of these keratinization disorders.

INTRODUCTION

Clinical and genetic heterogeneity of ichthyosis

Ichthyosis comprises a group of both acquired and heritable keratinization disorders characterized by hyperkeratotic and scaly skin (Brown and Irvine, 2008). Although the phenotypic spectrum of

ichthyosiform dermatoses is extremely broad, with either limited or extensive involvement of the skin, among the inherited forms, three clinically and genetically distinct subtypes have been identified: ichthyosis vulgaris, X-linked ichthyosis and lamellar ichthyosis (LI) (McGrath and Uitto, 2008; Brown and Irvine, 2008; Brown and McLean, 2008; Elias et al., 2004). LI in itself is a heterogeneous group of autosomal recessive disorders with large plaque-like brown scales over most of the body, associated with ectropion and alopecia.

Harlequin ichthyosis (HI) is a rare, extremely severe form of ichthyosis, most closely associated with the LI group of these disorders (Akiyama, 2006a). Neonates are born encased in a thick skin that not only restricts their movement, but also distorts their facial features, averting their lips and eyelids. Although newborns with HI frequently die within the first few days of life, a few of these affected individuals do survive, and their skin eventually resembles severe non-bullous congenital ichthyosiform erythroderma or LI.

HI is an autosomal recessive disorder caused by mutations in the ATP-binding cassette, sub-family A, member 12 (*ABCA12*) gene, which encodes a lipid transporter protein localized to lamellar granules in epidermal keratinocytes (Sakai et al., 2007). Mutations in the *ABCA12* gene result in congested lipid secretion and impaired barrier function of the stratum corneum (Kelsell et al., 2005). Thus, *ABCA12* is crucial to the development of the skin-lipid barrier in the stratum corneum.

An *Abca12*$^{-/-}$ mouse model has been vital in confirming the role of this transporter molecule in the skin abnormalities seen in HI, i.e. hyperkeratosis, impaired barrier function, abnormal lamellar bodies and the retention of lipid droplets in the epidermis (Yanagi et al., 2008; Smyth et al., 2008; Sundberg et al., 1997). The role of Abca12 in transporting lipids was confirmed by culturing keratinocytes from *Abca12*$^{-/-}$ mice and observing impaired lipid efflux leading to intracellular accumulation of lipids, specifically ceramides (Akiyama et al., 2005). However, the drawback of the mouse model is the long gestation period and small number of offspring per litter.

In addition to nonsyndromic variants, ichthyosis can be associated with clinical manifestations in a number of organ systems besides the skin. An example of syndromic ichthyoses is the CEDNIK syndrome, a rare autosomal recessive disorder with cerebral dysgenesis, neuropathy, ichthyosis and keratoderma. This syndrome has been shown to be associated with mutations in the *SNAP29* gene, which encodes soluble n-ethylmaleimide sensitive factor (NSF) attachment protein (SNAP)29, a member of the SNAP receptor (SNARE) family of proteins (Sprecher et al., 2005; Fuchs-Telem et al., 2011). SNARE proteins are required for vesicle trafficking and they mediate the fusion between the vesicles and their target membranes. *SNAP29* deficiency has been suggested to result in impaired maturation and secretion of lamellar granules, particularly interfering with the transport of lipids to stratum corneum; however, no animal model for the CEDNIK syndrome exists.

In an attempt to create an alternative, and perhaps more expedient, model system to study ichthyosis, we have performed work on zebrafish (*Danio rerio*), which has nearly the same complement of genes as mammals. Some of the benefits to working with zebrafish include their rapid development and the ease with which one can manipulate their gene expression by morpholino-based antisense oligonucleotides (Kari et al., 2007; Li et al., 2011). Zebrafish develop rapidly, with all major organs, including the skin, having developed by 5–6 days post-fertilization (dpf). They also produce a large number of embryos per laying, approximately 50–100 per female. In this study, we performed experiments to show that *abca12* and *snap29* gene knockdown in zebrafish causes epidermal changes that are similar, attesting to the concept that diverse pathogenetic pathways, as a result of mutations in different genes, can result in phenotypes in the spectrum of ichthyotic diseases. Thus, zebrafish provide a novel and expedient model system to study this group of devastating, currently intractable, diseases.

RESULTS

Identification of an *ABCA12*-related gene in the zebrafish genome

Search of the online gene database (NCBI) identified one human *ABCA12*-related sequence, *abca12*, which mapped to zebrafish chromosome 9. This zebrafish *abca12* gene had an open reading frame, and

all splice sites appeared intact, which allowed deduction of the intron-exon organization. The *abca12* gene consists of 53 exons, with sizes ranging from 55 to 2415 bp (Fig. 1A). The predicted primary sequence of the corresponding protein consists of 3634 amino acids, whereas the corresponding human primary sequence comprises 2595 amino acids. The overall conservation at the protein level was 49.3% and, consequently, the zebrafish *abca12* gene can be considered to be the human *ABCA12* homolog.

Alignment of human and zebrafish protein sequences revealed that zebrafish Abca12 has an extended 486 amino acid N-terminal sequence, as well as a number of insertions in the N-terminal half of the protein. However, alignment of zebrafish and human sequences identified conservation of domains that are characteristic of the ABC transporter proteins. Specifically, the zebrafish sequence, similar to the human sequence, was predicted to consist of four transmembrane domains (TMD1-4) and to contain two nucleotide binding fold domains (NBF1 and NBF2) (Tusnády et al., 2006) (Fig. 1A). The NBFs displayed characteristic sequences for Walker A and B motifs, as well as a highly conserved ABC signature sequence. Comparison of the deduced amino acid sequence within the NBF1 domain of zebrafish Abca12 showed 74% identity to the corresponding NBF1 domain in the human protein, whereas the NBF2 domain had 68% identity to human NBF2.

Evolutionary conservation of zebrafish *abca12*

Differences between the zebrafish *abca12* gene and homologous genes in other species were examined by phylogenetic analysis of the corresponding protein sequence by cladistic measurement (Fig. 1B). The cladogram suggested that the zebrafish gene is distant from most of the other *ABCA12*-related genes in a number of species, and, therefore, presumably diverged early. However, inclusion of other members of the ABC transporter family, such as ABCC10 and ABCC6, in different species, serving as an outgroup, indicated that the zebrafish Abca12 protein sequence is closer to human ABCA12 than it is to the sequences in the outgroup. To confirm that the zebrafish *abca12* is the correct ortholog of human *ABCA12*, syntenic analysis of *Abca12* in different species was performed (Fig. 1B). These analyses revealed that *ABCA12* and its flanking genes, *VWC2L* and *BARD1*, were located on the same chromosome in the same gene order in human, mouse, zebrafish and chicken genomes (Fig. 1B).

Expression of the zebrafish *abca12* gene during early embryonic development

The temporal expression profile of *abca12* was examined in embryos collected during the first 8 days of development, and the corresponding mRNA levels were determined by reverse transcriptase (RT)-PCR. An undetectable level of expression was noted in embryos at the time of fertilization [0 hours post-fertilization (hpf)], but detectable levels of mRNA transcripts were noted at 6 hpf, with a significant further increase by 1 dpf. During the subsequent days (2–8 dpf), the expression levels remained relatively constant in comparison with the control gene, *β-actin* (Fig. 2A).

Whole-mount in situ hybridization of *abca12* in zebrafish

To determine the spatial expression of *abca12* during different stages of zebrafish development, whole-mount in situ hybridization was performed using probes specific for the *abca12* gene (Fig. 2B). An antisense probe for *abca12* gave specific expression patterns. During the gastrula period, expression of *abca12* was observed in cells of the enveloping layer (EVL; Fig. 2B). Expression of the *abca12* gene in this tissue, which is named periderm after the end of gastrulation, is observed until the end of embryonic development. After 24 hpf, expression of *abca12* was also observed, although at lower levels, in the olfactory vesicle as well as in mucus-secreting cells (Fig. 2B). At the end of embryonic development, expression was observed mainly in olfactory vesicle, pharynx and mucus-secreting cells. A sense probe was used as a control and did not give a specific expression pattern.

Morpholino knockdown of *abca12* expression results in an altered skin phenotype

Morpholino antisense oligonucleotide (MO1) directed against a splice donor site in *abca12* was injected into one- to four-cell-stage embryos, and amplification of total RNA was performed by primers corresponding to exons 4 and 5. Using these primers, PCR amplification of *abca12* cDNA resulted in a 189 bp product, whereas amplification of genomic DNA generated a 356 bp product (Fig. 3A). RT-PCR of

total RNA extracted from zebrafish 3 days after injection with MO1 revealed that essentially all (>90%) of the pre-mRNA remained unprocessed, attesting to the efficiency of the morpholino knockdown (Fig. 3A). Injection of control morpholinos, either a global standard control MO (scMO) or 5-bp mismatched control (cMO), had no effect on pre-mRNA processing (Fig. 3A).

The effect of the injection of morpholinos into one- to four-cell embryos was first examined by determining the survival of the embryos. Of the 180 embryos injected with *abca12* MO1, 76% survived at 3 dpf, a number that did not statistically differ from the survival of embryos injected with standard control morpholino (81%) (Table 1). At 5 dpf, the survival of embryos injected with MO1 was only 6%, a statistically significant reduction from the survival noted with scMO and uninjected controls (81% and 87%, respectively; $P<0.0001$) (Table 1).

Examination of the morphology of zebrafish larvae injected with MO1 ($n=180$) revealed profound changes during development. Although no differences were noted between the morphant and control larvae at 1 dpf, by 3 dpf the morphants had developed noticeable changes in the distribution of pigment along their trunk and tail, in addition to pericardial edema (Fig. 4A). Upon careful examination at 3 dpf, 92% of larvae displayed yolk sac enlargement and severe disruption of their chromatophore distribution, with 75% exhibiting concomitant pericardial edema (Table 1).

Altered epidermal morphology in the morphant larvae

To examine the consequences of the morpholino-mediated knockdown of *abca12* expression in the skin of zebrafish, we first used scanning electron microscopy (SEM) to examine the surface contour and cellular morphology of the epidermis. In 3-dpf controls ($n=21$), well-demarcated keratinocytes with distinct borders and characteristic microridges were observed (Fig. 5). Examination of the skin surface of the morphant larvae ($n=4$) revealed perturbations in the architecture of the microridges, with spicules protruding from the center of each keratinocyte. Thus, the development of the top layer of skin during the first 3 days of zebrafish development was perturbed in the absence of Abca12 activity.

Alterations in the epidermis at 3 dpf were further examined by transmission electron microscopy (TEM) both in control and morphant larvae ($n=4$ in each group). At this developmental stage, normal epidermis consists of two unicellular layers, the superficial layer and the basal layer. The contour of the outer surface of the superficial layer is studded with spicules that correspond to the microridges noted previously on SEM (Fig. 6A). The epidermis rests on a basement membrane, which separates the epidermis from the underlying developing dermis.

The epidermis of the morphant larvae similarly consisted of two cell layers resting on a basement membrane (Fig. 6B). However, in contrast to the control larvae, both layers of the morphant epidermis contained an abundance of electron-dense granules, approximately 440 nm in average diameter. Closer examination of these aggregates at higher magnification suggested the presence of lipid-like vesicles within the larger electron-dense granules (Fig. 6C,D). It should be noted that, although somewhat similar aggregates of electron-dense material were noted in the epidermis of the control specimens, they were localized only to the area of the superficial layer just below the microridges.

Co-injection of human *ABCA12* mRNA rescues the morpholino-mediated phenotype

To test the specificity of the phenotypic changes associated with MO1 injection, a rescue experiment with co-injection of in vitro transcribed human *ABCA12* mRNA was performed. The injection of MO1 alone caused characteristic phenotypic changes, whereas co-injection of human mRNA together with MO1 partially rescued the phenotype (Fig. 4A,B). Specifically, at 5 dpf, the survival of the co-injected larvae was 62%, which is statistically different from the 6% in those injected with MO1 alone ($P<0.0001$) (Table 1). Also, 27% of co-injected larvae ($n=184$) had a phenotype that was indistinguishable from the controls. In the remaining 73% of co-injected larvae, the degree of yolk sac enlargement and chromatophore disorganization was noticeably less than in the larvae injected with MO1 alone. Of this 73%, 70% also manifested pericardial edema. The rescue experiment, in addition to injection of control morpholinos, attested to the specificity of the phenotype documented in the morphant larvae. These experiments also confirmed that the zebrafish *abca12* gene is the functional homolog of human *ABCA12*.

Epidermal perturbations in zebrafish injected with *snap29* morpholino

Because knockdown of *abca12* expression was speculated to interfere with lipid secretion by lamellar granules, resulting in a characteristic epidermal phenotype, we proceeded to test this postulate by interfering with the lipid transport by another, independent mechanism: knockdown of the expression of the *snap29* gene. The corresponding protein, Snap29, has been suggested to mediate lipid transport within the epidermis and the deficiency of SNAP29 expression results in syndromic ichthyosis in patients with CEDNIK syndrome (Rapaport et al., 2010; Sprecher et al., 2005).

Surveying the zebrafish genome database revealed the presence of one *SNAP29*-related gene, *snap29*, on chromosome 8. This gene product had 52% identity with the human gene product at the protein level, and cladogram and syntenic analyses suggested that zebrafish *snap29* is the ortholog of human *SNAP29* (Fig. 1C). The expression of the gene was readily detectable at 2 dpf by RT-PCR and the expression level increased during 3–8 dpf (Fig. 2C). In situ hybridization of larvae showed weak, ubiquitous expression with accentuation of the labeling in the central nervous system marginal zone (not shown).

Injection of a morpholino (MO2) placed on the exon-4–intron-4 junction of the *snap29* gene into one- to four-cell-stage embryos inhibited the processing of pre-mRNA by >90% (Fig. 3B). A second, non-overlapping morpholino (MO3), placed on the intron-4–exon-5 border of the *snap29* gene similarly resulted in >90% inhibition of the splicing of intron 4 (data not shown). Examination of the morphant larvae at 3 dpf (n=165 for MO2, and n=203 for MO3) revealed a phenotype consisting of pigmentary changes, somewhat analogous with those noted with the *abca12* morpholino, in 80% of larvae, and the contour of the epidermis in the tail section was irregular (Fig. 4C). SEM of 20 morphant larvae revealed perturbations in the morphology of the epidermis that were very similar to those noted as a result of *abca12* knockdown (Fig. 5). Examination of the epidermis of the *snap29* morphant larvae (n=4) by TEM at 3 dpf revealed an increase in vesicles, which appeared empty under the same fixation conditions that revealed accumulation of lipid-like material in *abca12* morphant fish (Fig. 6E,F). Thus, interference by morpholino knockdown of the expression of two independent genes, *abca12* and *snap29*, that are involved in lipid transport in the epidermis can lead to similar phenotypic alterations in the epidermal morphology.

DISCUSSION

ABCA12 mutations underlie HI

The molecular basis of HI is linked to mutations in the *ABCA12* gene (Akiyama et al., 2005; Kelsell et al., 2005). Initial approaches utilizing single-nucleotide polymorphism-based chip technology and homozygosity mapping of families with individuals affected with HI placed the candidate gene locus on chromosomal region 2q35, and microsatellite markers narrowed the interval to consist of six genes (Kelsell et al., 2005). Several previous observations pointed to *ABCA12* as a candidate gene within the critical region. First, a characteristic ultrastructural feature of the epidermis in HI is an abnormality in the localization of epidermal lipids, together with abnormal ultrastructural epidermal lamellar granules (Akiyama, 2006b). *ABCA12* has been suggested to encode a transmembrane transporter protein, which, from sequence homology with several other ABC family members, was thought to be involved in the transport of lipids (Kaminski et al., 2006). Second, the *ABCA12* gene was previously shown to harbor missense mutations in a milder form of ichthyosis, lamellar ichthyosis type 2 (LI2), with some resemblance to the phenotype in patients with HI who survive beyond the immediate postnatal period (Lefèvre et al., 2003). Currently, a total of 53 distinct mutations have been identified in the *ABCA12* gene (Akiyama, 2010).

Expression of *ABCA12* has been localized to lamellar granules. In normal epidermal keratinocytes there is an upregulation of *ABCA12* expression in association with physiological keratinization of the human epidermis (Sakai et al., 2007). Mutations in the *ABCA12* gene result in congested lipid retention in the skin of individuals with HI. It has been suggested that ABCA12 transports ceramides, the major lipid of the stratum corneum of the epidermis. Finally, lamellar-granule-mediated lipid secretion was resumed in the cultured keratinocytes of patients with HI upon transfer of the wild-type *ABCA12* gene (Akiyama

et al., 2005). Thus, it is clear that mutations in the *ABCA12* transporter gene underlie HI.

abca12 and zebrafish skin development

In this study, we have demonstrated that zebrafish *abca12* is the ortholog of human *ABCA12*. There is a high degree of conservation of the Walker A and B motifs in addition to the retention of the four transmembrane domains containing one, five, one and five transmembrane segments, respectively. Zebrafish NBF1 and NBF2 domains in the Abca12 protein have 74% and 68% similarity with human NBF1 and NBF2 domains, respectively, at the amino acid level.

Whole-mount in situ hybridization in developing zebrafish embryos revealed that *abca12* was expressed in the EVL and the periderm. The EVL first appears at the 64-cell stage of development (~2 hpf) and is the outermost monolayer of cells surrounding the embryo. The EVL eventually gives rise to the periderm, which is thought to ultimately be replaced by the superficial stratum of the epidermis (Kimmel et al., 1995; Le Guellec et al., 2004). Although the physiology of zebrafish skin is still largely unexplored, the fact that *abca12* is expressed in the skin suggests its importance in normal skin development. This hypothesis is further strengthened by the results from our morpholino experiments. Injecting a morpholino that inhibited pre-mRNA splicing by >90% produced alterations in chromatophore distribution and the abnormal retention of lipids in both layers of the epidermis. Not only does this suggest that *abca12* is responsible for lipid transport in zebrafish, but the abnormal accumulation of lipids throughout the epidermis is a frequent finding in individuals with HI. Finally, the rescue of this phenotype by co-injection of human *ABCA12* mRNA shows that the phenotype is the result of *abca12* knockdown and not due to an off-target effect. In this context, it should be emphasized that the EVL-derived skin in zebrafish is embryologically different from the mammalian skin. Specifically, zebrafish epidermis does not undergo terminal differentiation, which in human skin culminates in the development of stratum corneum with barrier function. Emphasizing this difference is the fact that survey of the current zebrafish genome database (Ensembl, Zebrafish Zv9; http://www.ensembl.org/Danio_rerio/Info/Index) does not reveal the presence of filaggrin, involucrin and trichohyalin genes, which are crucial for development of the stratum corneum in human epidermis (Li et al., 2011).

The role of lipids in epidermal development is further emphasized by our findings that knockdown of the expression of an independent gene, *snap29*, results in a similar epidermal phenotype as noted in *abca12* mutant larvae. Snap29 has been postulated to mediate lipid transport in the epidermis by facilitating membrane fusion of lamellar granules (Sprecher et al., 2005). Thus, interference of lipid trafficking by knockdown of two independent genes results in phenocopies of the epidermal perturbations in zebrafish, mimicking epidermal alterations in different forms of ichthyosis. It should be noted that, similar to the CEDNIK syndrome, ichthyosis has been reported in association with mental retardation, enteropathy, deafness, peripheral neuropathy and keratodermia, dubbed as the MEDNIK syndrome (Montpetit et al., 2008). This constellation was shown to be associated with a homozygous splice-site mutation in the *AP1S1* gene, encoding a subunit of the adaptor protein complex that regulates clathrin-coated vesicle assembly, protein cargo sorting, and vesicular trafficking between organelles in eukaryotic cells (Montpetit et al., 2008). The pathogenic effect of this mutation was validated by knockdown of *ap1s1* expression in zebrafish by a morpholino, resulting in perturbation in skin formation, reduced pigmentation and motility deficits. These findings, together with our observations in *snap29* mutant larvae, attest to the importance of vesicular trafficking in epidermal morphogenesis.

As indicated by morphological observations of the developing epidermis in zebrafish in comparison with human skin, there are clear differences. For example, the embryological origin of the EVL (periderm) in zebrafish is distinct from the basal layer in embryonic skin. In spite of this difference, there is an increasing body of evidence suggesting that the underlying molecular differentiation pathways are conserved between mammals and the zebrafish epidermis, based on molecular homologies (Sabel et al., 2009; Slanchev et al., 2009). Our work highlighting the early *abca12* expression in the EVL seems to support the conclusions that EVL forms the external layer of the embryonic and larval dermis and represents the initial differentiation of a true epidermis (Fukazawa et al., 2010).

Collectively, our results highlight the role of lipid transport and vesicular trafficking in epidermal

development, and the results further suggest that zebrafish can serve as a model system to study different variants of ichthyosis, such as HI and the CEDNIK syndrome. Besides increasing our understanding of the disease mechanisms involved in ichthyotic syndromes, this model system is potentially useful for testing novel treatment modalities, for example by performing a small molecule library screen for compounds that are able to suppress the phenotype.

METHODS

Maintenance of zebrafish

Adult wild-type zebrafish were maintained under standard conditions at 28.5°C. Zebrafish embryos and larvae were also maintained at 28.5°C in a special embryo medium. All animals were housed in the zebrafish facility at Thomas Jefferson University and were cared for and used in accordance with University Institutional Animal Care and Use Committee guidelines and permission.

Phylogenetic and syntenic analyses

The genomic sequences of zebrafish were extracted from the Ensembl database. The zebrafish protein sequences were aligned with the corresponding proteins in different species by using ClustalW software (http://www.ebi.ac.uk/clustalw/).

The accession numbers for the *abca12* gene products in different species are: *E. caballus* (ENSECAP00000007797), *C. lupus familiaris* (XP_536058), *B. taurus* (XP_001788086), *H. sapiens* (NP_775099), *P. troglodytes* (XP_516070), *M. musculus* (XP_001002308), *R. norvegicus* (XP_237242), *G. gallus* (XP_421867), *D. rerio* (XP_686632) and *O. latipes* (ENSORLP00000020129). The accession numbers for *ABCC10* in *H. sapiens* is NP_258261. The accession numbers for *Abcc6* in different species are: *M. musculus* (NP_061265), *H. sapiens* (NP_001162), *D. rerio* (ENSDARP00000065432), *T. nigroviridis* (ENSTNIP00000015029) and *T. rubripes* (ENSTRUP00000029065).

The accession numbers for the *snap29* gene products in different species are: *H. sapiens* (NP_004773.1), *P. troglodytes* (XP_514997.2), *M. mulatta* (XP_001086227.1), *M. musculus* (NP_075837.3), *R. norvegicus* (NP_446262.3), *C. familiaris* (XP_543568.2), *B. taurus* (NP_001069427.1), *G. gallus* (NP_001025823.1), *D. rerio* (XP_700124.3), *S. salar* (NP_001134759.1), *X. laevis* (NP_001080076.1) and *A. thaliana* (NP_196405.1).

Phylogenetic analyses were conducted in the Molecular Evolution Genetics Analysis software (MEGA) version 4.0 (Tamura et al., 2007). The cladogram was constructed using the Neighbor-Joining method (Saitou and Nei, 1987). The Kimura two-parameter method was used to compute the evolutionary distances (Zuckerkandl and Pauling, 1965). The statistical reliance of NJ tree branches was evaluated using 1000 bootstrap samples.

For syntenic analysis, the orientation and chromosomal positions of *abca12* and *snap29* and their adjacent genes were determined manually from the gene orientations in the current Ensembl database. The zebrafish (Zv9), human (GRCh37/hg19), mouse (NCB137/mm9) and chicken (WUGSC2.1/galGal3) genome assembly versions were used for this analysis.

In situ hybridization

Whole-mount in situ hybridization was performed as described previously (Thisse and Thisse, 2008). Collected zebrafish embryos were fixed in 4% paraformaldehyde before hybridization. Digoxigenin (DIG)-labeled antisense and sense probes were synthesized. After hybridization, detection was performed with an anti-DIG antibody coupled to alkaline phosphatase.

Morpholinos and microinjection

Morpholino oligonucleotides were obtained from Gene Tools, LLC (Corvalis, OR). The morpholino oligomer sequences were written from 5′ to 3′, to correspond to the following genomic sequences (brackets surround the morpholino target sequence, exon sequences are capitalized, intron sequences

are in lowercase, and nucleotide substitutions are bolded). For *abca12* knockdown: splice donor site morpholino (MO1), tgggaaataaatgtaatttacctgt, targets the exon-4–intron-4 junction, AAATGAAATAACTGA[ACAGgta-aattacatttatttccca]acggtc; 5-base pair mismatched control morpholino for *abca12* (cMO): tgg**c**aaa**a**aaat**c**taatttac**gt**c**t**. For *snap29* knockdown: splice donor site morpholino (MO2), ctgctcttgtgtttctcacccaggt, targets the exon-4–intron-4 junction, GACAGAA[ACCTGGgtgagaaacacaagacag]cttctctcata; a second *snap29* splice junction morpholino (MO3) targets the intron 4-exon 5 border, ctcatctggaggacacaaacacaca, agtgtgtgtg[tgtgtg-tttgtgtcctccagAT GAG]ATGTCTCTGGGTC. Global standard control morpholino (scMO), cctcttacctcagttacaatttata, has no target sequence in the zebrafish genome and is, therefore, inactive.

Embryos at the one- to four-cell stage were injected with an *abca12* morpholino (MO1, 25.6 ng) or *snap29* morpholinos (MO2, 2.6 ng and MO3, 5.2 ng) using glass microelectrodes fitted to a gas pressure injector (PL1-100, Harvard Apparatus). Electrodes were pulled (P-97, Flaming/Brown) and filled with morpholino and phenol red (final concentration 0.025%) to visualize the injected embryos. The embryos were then followed for viability, morphology and mRNA expression levels.

Total RNA isolation and cDNA synthesis

Zebrafish embryos were collected at 0 as well as 6 hpf and 1–8 dpf. They were disintegrated by pipetting through a 21 gauge needle and total RNA was extracted using TRIzol reagent (Invitrogen, Carlsbad, CA). To remove contaminating genomic DNA, RNase-free DNase I digestion (Fisher Scientific, St Louis, MO) was performed. 1 μg of total RNA was reverse transcribed using the Superscript III First-Strand cDNA synthesis kit (Invitrogen) according to the manufacturer's protocol. Controls were performed by omitting the reverse transcriptase enzyme. All cDNA samples were stored at −20°C for future use.

PCR amplification of cDNA

abca12 cDNA was amplified by PCR using a forward primer on exon 4 (5′-ATCTGGGACAACTTGGGCAACT-3′), and a reverse primer on exon 5 (5′-TCATCTGGTCAGCAGTTCCAGAGA-3′). The *snap29* cDNA was amplified using a forward primer on exon 4 (5′-TTCTGCTGCTCTTGATAACGGCT-3′), and a reverse primer on exon 5 (5′-TTTAAGGCTTTTGAGCTGCCGGTT-3′). Primers for the zebrafish *β-actin* gene (fwd: 5′-ATCTGGCACCACACCTTCTACAATG; rev: 5′-GGGGTG-TTGAAGGTCTCAAACATGAT) were used as a positive control. PCR was performed using Taq polymerase and Q buffer (Qiagen, Valencia, CA), according to the manufacturer's instructions. The PCR conditions were as follows: an initial denaturation at 94°C for 5 minutes, followed by 35 cycles of 94°C for 1 minute; 58°C for 1 minute; 72°C for 1 minute; and finally 72°C for 10 minutes. The intensity of the bands was quantified using ImageQuant version 5.0 software (Molecular Dynamics, Sunnyvale, CA).

mRNA rescue experiments

Capped full-length human mRNA corresponding to *ABCA12* was transcribed from an expression vector pCMV-Tag4B using the T3 mMessage mMachine kit (Ambion, Austin, TX). The morpholino was injected into one- to four-cell-stage embryos either alone or in combination with mRNA (2.3 ng) and followed for viability and morphology.

Scanning electron microscopy

Samples were fixed in neutral buffered formalin at room temperature for 2 hours, followed by a rinse with phosphate buffered saline and an ethanol dehydration series of exchanges by completely replacing each successively higher ethanol solution with the next higher (20, 30, 50, 75, 95 and 100%). Samples were then incubated for 15 minutes in a 1.5 ml micro test tube containing 1,1,2-Trichloro-1,2,2-trifluoroethane before covering the open micro test tube with parafilm, punching holes in it with a 30G needle, and situating it under a fume hood where it was dried by turbulent air flow. Samples were then mounted onto stubs with carbon paint and coated in 50 nm of gold using a sputter coater. Specimens were imaged in a JEOL-T330A scanning electron microscope (JEOL, Tokyo, Japan) at 15 kV.

Transmission electron microscopy

Samples were collected and fixed overnight at 4°C in 2.5% gluteraldehyde, 2% paraformaldehyde and 0.1 M sodium cacodylate. Samples were then washed in 0.1 M sodium cacodylate before undergoing secondary fixation in 2% osmium tetroxide, 1.5% potassium ferricyanide and 0.1 M sodium. Samples were again washed with 0.1 M sodium cacodylate followed by deionized water before undergoing en block staining with 2% uranyl acetate. Samples were washed again with deionized water, then dehydrated in a graded ethanol series and embedded in EMbed-812 (EMS, Hatfield, PA). Ultrathin sections (60 nm) were cut and analyzed using a JEOL JEM-1010 transmission electron microscope fitted with a Hamamatsu digital camera (Hamamatsu Photonics, Hamamatsu City, Japan) and AMT Advantage image capture software (AMT, Danvers, MA).

Statistical analysis

Risk differences and 95% confidence intervals were calculated between experimental groups with regards to survival, skin phenotype and edema in Table 1, for 3 dpf and 5 dpf separately. Fisher's exact test was used to determine the difference between proportions because of the presence of cells with zero observations. Adjustments for multiple comparisons were performed using False Discovery Rate, and it is these adjusted *P*-values that are reported. Analyses were conducted using SAS 9.2 (SAS Institute, Cary, NC).

TRANSLATIONAL IMPACT

Clinical issue

Ichthyosis comprises a group of cutaneous disorders characterized by dry, scaly skin and a broad spectrum of other phenotypic manifestations. One of the most severe forms of ichthyosis is known as harlequin ichthyosis (HI); neonates affected with HI are born encased in a thick skin that restricts their movement and frequently die shortly after birth. Some forms of ichthyosis are syndromic; for example, CEDNIK syndrome is so-named because it consists of cerebral dysgenesis, neuropathy, ichthyosis and keratoderma. Details of the pathomechanisms of HI have recently been revealed through molecular genetics, which showed that patients with this disorder carry mutations in the *ABCA12* gene. Examination of *Abca12*$^{-/-}$ mice suggested that this gene encodes a transmembrane transporter present in the epidermis that is postulated to transport lipids (specifically ceramides) and that is required for formation of the stratum corneum on the surface of the skin. Although the mouse model is useful in that it recapitulates features of human HI, drawbacks include the long gestational period and the small number of offspring produced per litter. CEDNIK syndrome is caused by mutations in the *SNAP29* gene, which is required for normal vesicle trafficking and lipid transport in the epidermis. There is no animal model for this syndrome.

Results

To create alternative, more expedient model systems to investigate pathological mechanisms of both HI and CEDNIK syndrome, the authors of this study knocked down the homologs of *ABCA12* and *SNAP29* in zebrafish embryos (*Danio rerio*). Morpholino antisense oligonucleotides targeted to exon-intron splice junctions were used to inhibit the splicing of *abca12* or *snap29* pre-mRNA. Inhibition of processing of either one of these mRNAs was accompanied by changes in the distribution of pigment along the trunk and tail of the fish as early as 2 days post-fertilization (dpf). Examination of epidermal morphology by scanning electron microscopy revealed perturbations in the surface contour of the keratinocytes, with loss of characteristic microridges and development of pathological spicules protruding from the center of each keratinocyte. These epidermal changes were accompanied by premature demise of the fish by 5 dpf. Transmission electron microscopy revealed an abundance of electron-dense granules in both morphants: lipid-like vesicles were seen in *abca12* knockdown fish, whereas the epidermis of *snap29* knockdown animals showed the presence of apparently empty vesicles.

Implications and future directions

This study demonstrates that inhibition of *abca12* or *snap29* gene splicing in zebrafish leads to epidermal perturbations that are similar to those seen in human patients with various forms of ichthyosis. In addition, it suggests that interfering with two independent pathways involved in lipid transport can result in phenotypically similar perturbations in epidermal morphogenesis. These systems can serve as models to study ichthyosis, and provide a means to develop pharmacological approaches towards treatment of this currently intractable group of diseases. Finally, in a broader sense, this study attests to the feasibility of using zebrafish as a model system to study heritable skin diseases.

Acknowledgments

The authors thank the following colleagues for advice and assistance: Wolfgang Driever, Institute for Biology I, University of Freiburg; Raymond Meade, Biomedical Imaging Core Facility, University of Pennsylvania; Gerald Harrison, Department of Biochemistry, School of Dental Medicine, University of Pennsylvania; Jean-Yves Sire, Equipe "Evolution et Développement du Squelette", Université Paris; Eijiro Adachi, Department of Matrix Biology and Tissue Regeneration, Graduate School of Medical Sciences, Kitasato University; Ulrich Rodeck, Gabor Kari, April Aguillard, Adele Donahue and Andrzej Fertala, Department of Dermatology and Cutaneous Biology, Thomas Jefferson University; Terry Hyslop and Jocelyn Andrel, Department of Pharmacology and Experimental Therapeutics, Thomas Jefferson University. Carol Kelly assisted in manuscript preparation. This study was supported by the NIH/NIAMS grant R01AR055225 to J.U.; by the University of Virginia to C.T. and B.T. Q.L. is a recipient of a Research Career Development Award from the Dermatology Foundation.

Footnotes

COMPETING INTERESTS

The authors declare that they do not have any competing or financial interests.

AUTHOR CONTRIBUTIONS

Q.L., M.F., C.T. and B.T. performed the experiments; M.A. provided reagents; H.S. and E.S. interpreted the data and edited the manuscript; S.-Y.H. contributed to the data analysis; J.U. developed the concept, interpreted the data and prepared the manuscript.

REFERENCES

Akiyama M. (2006a). Harlequin ichthyosis and other autosomal recessive congenital ichthyoses: the underlying genetic defects and pathomechanisms. J. Dermatol. Sci. 42, 83–89. [PubMed: 16481150]

Akiyama M. (2006b). Pathomechanisms of harlequin ichthyosis and ABCA transporters in human diseases. Arch. Dermatol. 142, 914–918. [PubMed: 16847209]

Akiyama M. (2010). *ABCA12* mutations in harlequin ichthyosis, congenital ichthyosiform erythroderma and lamellar ichthyosis. Hum. Mutat. 31, 1090–1096. [PubMed: 20672373]

Akiyama M., Sugiyama-Nakagiri Y., Sakai K., McMillan J. R., Goto M., Arita K., Tsuji-Abe Y., Tabata N., Matsuoka K., Sasaki R. (2005). Mutations in lipid transporter ABCA12 in harlequin ichthyosis and functional recovery by corrective gene transfer. J. Clin. Invest. 115, 1777–1784. [PMCID: PMC1159149] [PubMed: 16007253]

Brown S. J., Irvine A. D. (2008). Atopic eczema and the filaggrin story. Semin. Cutan. Med. Surg. 27, 128–137. [PubMed: 18620134]

Brown S. J., McLean W. H. I. (2008). Eczema genetics: current state of knowledge and future goals. J. Invest. Dermatol. 129, 543–552. [PubMed: 19209157]

Elias P. M., Crumrine D., Rassner U., Hachem J. P., Menon G. K., Man W., Choy M. H., Leypoldt L., Feingold K. R., Williams M. L. (2004). Basis for abnormal desquamation and permeability barrier dysfunction in RXLI. J. Invest. Dermatol. 122, 314–319. [PubMed: 15009711]

Fuchs-Telem D., Stewart H., Rapaport D., Nousbeck J., Gat A., Gini M., Lugassy Y., Emmert S., Eckl K., Hennies H. C., et al. (2011). CEDNIK syndrome results from loss-of-function mutations in